

# Optical properties of electrostatically assembled films of CdS and ZnS colloid nanoparticles

Suryajaya<sup>1</sup>, A. Nabok<sup>1</sup>, F. Davis<sup>2</sup>, A. Hassan<sup>1</sup>, S.P.J. Higson<sup>2</sup> and J. Evans-Freeman<sup>1</sup>

E-mail: s.suryajaya@shu.ac.uk

**Abstract.** This work presents a cost-effective technology for the formation of nanostructured semiconductor materials for tunable light emitting devices. CdS and ZnS semiconducting colloid nanoparticles coated with organic shell, containing either  $\text{SO}_3^-$  or  $\text{NH}_3^+$  groups, were deposited as thin films using the technique of electrostatic self-assembly. The films produced were characterized with UV-vis spectroscopy, spectroscopic ellipsometry, and AFM. UV-vis spectra show a substantial blue shift of the main absorption band of both CdS and ZnS containing films with respect to the bulk materials, due to the phenomenon of quantum confinement. The nanoparticles' radius of 1.8 nm, evaluated from the spectral shift, corresponds well to the film thickness obtained by ellipsometry. AFM shows the formation of larger aggregates of nanoparticles on solid surfaces.

Keywords: CdS, ZnS, colloid nanoparticles, electrostatic self-assembly, quantum confinement, ellipsometry, AFM

## 1. INTRODUCTION

In the past decade, II-VI semiconductor nanoparticles have attracted much attention because of their size-dependent (and thus tunable) photo- and electro- luminescence properties and promising applications in optoelectronics. Different chemical (or wet) techniques for the preparation and deposition of II-VI semiconductor nanoparticles, such as LB film method [1,2], Electrochemical Deposition [3,4] and Electrostatic Self-assembly of colloid nanoparticles [5-10], have been exploited. The latter method is of particular interest, because it allows the deposition of pre-synthesized colloid nanoparticles of different II-VI semiconducting materials. The main absorption and luminescent bands of such materials can be easily controlled by their composition and particle size to enable the fabrication of LEDs of required colours [10] or white light LEDs covering the whole visible spectral range [7].

The main purpose of this research is to provide convenient, economic, and environmental friendly alternatives to some of the expensive physical methods of nano-structures formation. In this work, we use an aqueous-phase synthesis of colloid nanoparticles', similar to the route described in [11]. A small modification of the synthesis allowed us to produce CdS and ZnS colloid nanoparticles coated with organic shell containing either  $\text{SO}_3^-$  or  $\text{NH}_3^+$  groups and thus suitable for electrostatic self-assembly (ESA). This gives more possible deposition procedures by alternating the layers of cationic and anionic nanoparticles with the polycations and polyanions, respectively, as well as a route to deposit nanoparticles even without intermediate binding polyelectrolyte layers. This approach could be useful in the future for the formation of semiconductor superlattices.

This work focused on the optimization of the film deposition procedure and studying optical properties of thin films containing II-VI nanoparticles using UV-visible absorption spectroscopy and spectroscopic ellipsometry. The morphology of the obtained films was assessed using tapping mode atomic force microscopy (AFM).

## 2. EXPERIMENTAL DETAILS

---

<sup>1</sup> Materials and Engineering Research Institute, Sheffield Hallam University, City Campus, Pond Street, Sheffield, S1 1WB, UK

<sup>2</sup> Cranfield Health, Cranfield University, Silsoe, Bedfordshire, MK45 4DT, UK.

### 2.1. Preparation of colloid nanoparticles

CdS-SO<sub>3</sub><sup>-</sup> and ZnS-SO<sub>3</sub><sup>-</sup> colloid nanoparticles were prepared by mixing aqueous solutions of 0.04 M sodium 2-mercapto-ethane-sulfonate with 0.04 M solution of either CdCl<sub>2</sub> or ZnCl<sub>2</sub>. A 0.04 M solution of sodium sulfide was then added dropwise to the solution while it is stirred. Colloid nanoparticles of CdS-NH<sub>2</sub><sup>+</sup> and ZnS-NH<sub>2</sub><sup>+</sup> were made the same way but using 0.04 M cysteamine hydrochloride as a capping agent.

All chemicals used were of high purity purchased from Sigma-Aldrich. Solutions were prepared using Millipore water having resistance of no less than 18 MΩ.

### 2.2. Electrostatic self-assembly

The films of CdS and ZnS nanoparticles coated with either negatively (SO<sub>3</sub><sup>-</sup>) or positively (NH<sub>2</sub><sup>+</sup>) charged shells were deposited layer-by-layer onto electrically charged solid substrates using intermediate layers of either polyanions, such as poly-allylamine hydrochloride (PAH), or polycations, such as poly-styrene-sulfonate sodium salt (PSS) [5,6]. The substrates (glass and quartz slides, and silicon wafers) were treated in 1% KOH solution in 60% ethanol, to make them negatively charged [12].

Multilayers of CdS-SO<sub>3</sub><sup>-</sup> and ZnS-SO<sub>3</sub><sup>-</sup> nanoparticles, were deposited by dipping the substrate consecutively into 1M PAH solution and then into respective colloid solution for 10 minutes in each, as shown in Figure 1(a).

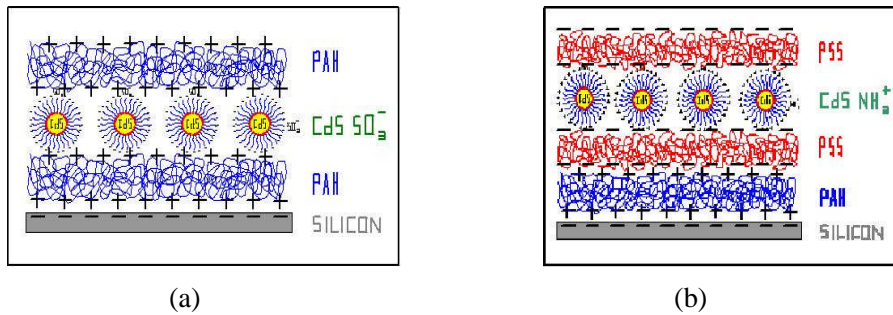


Figure 1. Deposition of colloid nanoparticles CdS-SO<sub>3</sub><sup>-</sup> (a) and CdS-NH<sub>2</sub><sup>+</sup> (b).

Multilayers of CdS-NH<sub>2</sub><sup>+</sup> and ZnS-NH<sub>2</sub><sup>+</sup> nanoparticles, were prepared by dipping the substrate firstly into 1M PAA for 20 min followed by consecutive dipping in 1M PSS solution and in respective colloid solution for 10 min in each, as shown in Figure 1(b). All samples were thoroughly rinsed in Millipore water after each deposition step.

### 2.3. Experimental methods

UV-visible absorption spectra of the films deposited onto glass and quartz substrates were recorded using Varian CARY 50 spectrophotometer. In the case of ZnS particles which, have a main absorption band at a much shorter wavelength range, quartz substrates were used.

Optical parameters of the films obtained were studied with spectroscopic ellipsometry. The measurements were carried out on the films deposited on pieces of silicon wafers using the J.A. Woollam M2000V rotating analyser spectroscopic instrument, which operates in the spectral range of 370-1000 nm. The angle of incidence of 70° was used. The optical parameters, i.e. thickness ( $d$ ) and complex refractive index ( $N = n - jk$ ), where  $n$  is the index of refraction and  $k$  is the extinction coefficient were evaluated from the experimental spectra of two ellipsometric parameters  $\Psi$  and  $\Delta$  representing, respectively, the amplitude ratio and phase shift between  $p$ - and  $s$ - components of polarised light:

$$\Psi = \arctan(A_p/A_s), \quad \Delta = \varphi_p - \varphi_s \quad (1)$$

The procedure of fitting of the experimental  $\Psi(\lambda)$  and  $\Delta(\lambda)$  spectra consist of solving the main ellipsometric equation

$$\tan(\Psi) \exp(i\Delta) = \frac{R_p}{R_s}, \quad (2)$$

in which Fresnel reflection coefficients,  $R_p$  and  $R_s$  for  $p$ - and  $s$ - components of polarized light, respectively, are related to the parameters of the reflecting system ( $d$ ,  $n$ , and  $k$ ) through Fresnel equations [13]. Commercial VWASE32® software provided by J.A. Woollam Co [14] was used for data fitting.

The morphology of the films deposited on silicon substrates was studied with AFM using the Digital Instruments Nanoscope IIIa equipment. Typical parameters for tapping mode measurements were: cantilever oscillation frequency of 300-500 kHz, VEECO tapping mode cantilevers with the tip radius less than 10 nm, the scan rate of 1 Hz. Particle size analysis of the obtained images was performed using the Digital Instruments integrated image processing software.

### 3. RESULTS AND DISCUSSION

Typical absorption spectra of CdS and ZnS nanoparticles embedded in organic films of PAH and PSS are shown in Figures 2 (a) and (b). The absorption intensity increases monotonically with the increase in the number of layers, which reflects the consistency of electrostatic deposition. It has to be noted that the role of polyelectrolyte layers is crucial for successful deposition. The attempts of alternative deposition of layers of anion and cation modified nanoparticles without intermediate polyelectrolyte layers failed because the first layer peeled off during the attempted deposition of the second layer. This was most likely because of a poor adhesion of the first layer of nanoparticles to the substrate. In the spectra presented in Fig. 2 and 3 the main absorption bands were found at 405 nm for CdS, and 290 nm for ZnS. Both of them are blue shifted from the respective absorption bands of 512 nm and 335 nm for bulk CdS and ZnS materials. This is believed to be due to the effect of quantum confinement. The size of nanoparticles can be evaluated from the values of blue shift of the absorption bands [1, 15]. Similar spectra were observed for CdS and ZnS nanoparticles capped with  $\text{NH}_2^+$  groups.

In order to obtain the exact positions of absorption maxima, Gaussian fitting of absorption spectra re-plotted in energy coordinates was performed similar to [16] and shown in Figures 3 (a) and (b). The observed energy dispersion may reflect the combination of the size distribution of nanoparticles and the presence of higher index energy levels of size quantization. Only the first maximum (in each spectrum) corresponding to the ground state level was chosen for further analysis.

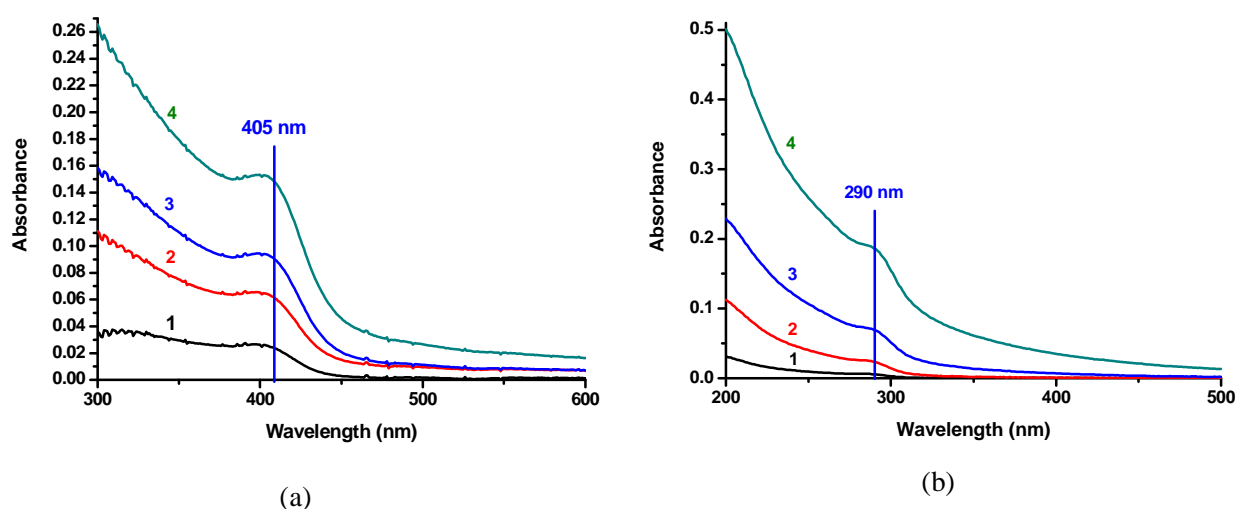


Figure 2. UV-vis absorption spectra of PAH/CdS-SO<sub>3</sub><sup>-</sup> film (a) and PAH/ZnS-SO<sub>3</sub><sup>-</sup> film (b). The numbers near respective spectra correspond to the number of polyelectrolyte/nanoparticle bilayers.

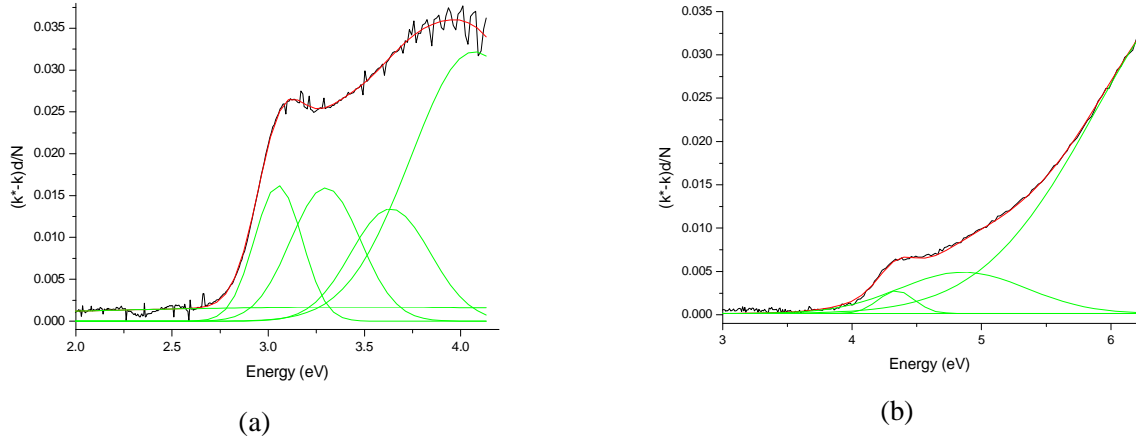


Figure 3. Gaussian fitting of the spectra of the first layer of CdS-SO<sub>3</sub><sup>-</sup> (a) and the first layer of ZnS-SO<sub>3</sub><sup>-</sup> (b).

The radius of semiconductor clusters can be calculated using Efron equation for the energy spectrum in nanoparticles of direct band gap semiconductors, having parabolic  $E(k)$  dispersion, in the case of strong confinement, when the particles are smaller than Bohr exciton radius [16].

$$E_{(n,l)} = E_g + \frac{\hbar^2}{2\mu R^2} \phi_{(n,l)}^2 \quad (3)$$

Here  $E_g$  is the band gap for bulk semiconductors,  $\mu$  is the reduced effective mass of exciton,  $\frac{1}{\mu} = \frac{1}{m_e^*} + \frac{1}{m_h^*}$ , and

$\phi_{(n,l)}$  are routes of Bessel functions (for the ground state  $\phi_{(0,1)} = \pi$ ). The obtained values of particle size are summarized in Table 1.

**Table 1.** The results of Gaussian fitting of the absorption spectra of CdS and ZnS nanoparticles.

	E (eV)	Radius (nm)
CdS SO <sub>3</sub> <sup>-</sup>	3.12 ± 0.0086	1.8
CdS NH <sub>2</sub> <sup>+</sup>	3.08 ± 0.0020	1.84
ZnS SO <sub>3</sub> <sup>-</sup>	4.27 ± 0.0026	1.9
ZnS NH <sub>2</sub> <sup>+</sup>	4.38 ± 0.0074	1.8

Spectroscopic ellipsometry measurements confirmed the growth of polyelectrolyte/nanoparticles films on silicon. For example, the series of  $\Delta(\lambda)$  spectra in Figure 4 show their consecutive shift downwards after each layer being deposited, which corresponds to the increase in the film thickness.

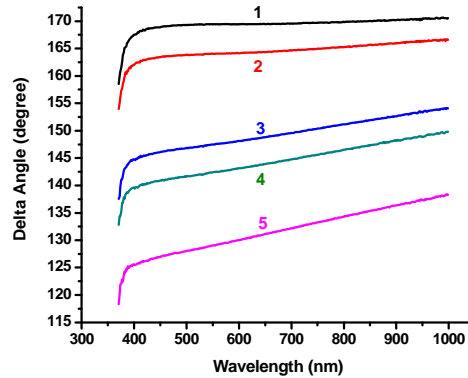


Figure 4. Typical  $\Delta(\lambda)$  ellipsometric spectra of silicon substrate (1), and consecutively deposited on top layers:

1<sup>st</sup> layer of PAH (2), 1<sup>st</sup> layer of ZnS nanoparticles (3), 2<sup>nd</sup> layer of PAH (4), 2<sup>nd</sup> layer of ZnS nanoparticles (5). The inset shows the model for ellipsometry data fitting.

Fitting the experimental  $\Psi$  and  $\Delta$  ellipsometric spectra using VWASE@ J.A. Woollam software allowed the extraction of optical parameters, such as the thickness ( $d$ ) refractive index ( $n$ ) and extinction coefficient ( $k$ ) of all consecutively deposited layers. A multilayer model used for ellipsometry fitting, shown in Tables 2 and 3, consists of Si substrate, SiO<sub>2</sub> layer representing a very thin (2-3 nm) film of native oxide, polyelectrolyte films of either PAH or PSS represented by Cauchy model, and the layers of either CdS or ZnS nanoparticles. The file names of models chosen from the VWASE32® library are shown near respective layers in Tables 2 and 3. The default medium (air) was used everywhere. The parameters of all layers were obtained by fitting the spectra for consecutively deposited layers and fixing the previously obtained parameters for the layers below. For the transparent dielectric layers of polyelectrolyte (PAH or PSS) the value of  $k = 0$  was fixed and the variables were the thickness ( $d$ ) and the parameter  $A$  in the Cauchy dispersion model [14]:

$$n = A + B/\lambda^2 + C/\lambda^4 \quad (4)$$

For the layers of CdS and ZnS nanoparticles the model files of respective bulk materials were used, and all three parameters  $d$ ,  $n$ , and  $k$  were varied during fitting.

The results of fitting are summarized in Tables 2 and 3. Although the whole spectra of  $n$  and  $k$  were obtained, only the values at 633 nm are shown. The obtained thicknesses of nanoparticle layers of around 5 nm for both CdS and ZnS correspond well to size of particles evaluated from UV-vis spectral data taking into account an additional thickness of the organic shell. The obtained larger thickness of the 2nd layer of CdS nanoparticles (in Table 2) is most likely due to the aggregation of nanoparticles. The obtained values of  $n$  and, particularly,  $k$  deviate from the respective values of bulk materials ( $n = 2.475$ ,  $k = 0.0186$  for CdS and  $n = 2.364$ ,  $k = 0.0077$  for ZnS). This may be attributed to the substantial increase in the oscillator strength due to the effect of quantum confinement [15]. The obtained values of refractive index for polyelectrolyte layers of 1.49 - 1.54 are quite typical for PAH and PSS films, while the thickness of around 2 nm is slightly larger than reported previously [12], which may be caused by inhomogeneous coating.

**Table 2.** Ellipsometry fitting of for PAH/CdS-SO<sub>3</sub><sup>-</sup> films

Layer	d (nm)	n (at 633 nm)	k (at 633 nm)
Si ( <i>Si_gel.mat</i> )		3.867	0.02
SiO <sub>2</sub> ( <i>SiO2.mat</i> )	5.99 ± 0.03	1.46	0
PAH ( <i>CAUCHY.mat</i> )	1.94 ± 0.03	1.49	0
1 <sup>st</sup> CdS ( <i>CDSO.mat</i> )	4.94 ± 0.04	2.28	0.74
PAH ( <i>Cauchy</i> )	2.12 ± 0.02	1.54	0
2 <sup>nd</sup> CdS ( <i>CDSO.mat</i> )	12.84 ± 0.02	1.82	0.74

**Table 3.** Ellipsometry fitting of for PAH/ZnS-SO<sub>3</sub><sup>-</sup> films

Layer	d (nm)	n (at 633 nm)	k (at 633 nm)
Si ( <i>Si_gel.mat</i> )		3.867	0.02
SiO <sub>2</sub> ( <i>SiO2.mat</i> )	3.53 ± 0.05	1.46	0
PAH ( <i>CAUCHY.mat</i> )	1.96 ± 0.06	1.49	0
1 <sup>st</sup> ZnS ( <i>ZNS.mat</i> )	5.24 ± 0.03	2.29	0.78
PAH ( <i>CAUCHY.mat</i> )	2.24 ± 0.01	1.49	0
2 <sup>nd</sup> ZnS ( <i>ZNS.mat</i> )	5.53 ± 0.06	2.29	0.78

Typical tapping mode AFM images of consecutively deposited layers of polyelectrolytes and colloid nanoparticles are shown in Figures 5 and 6. The first PAH layer in Fig. 5 shows non-complete surface coverage. The next layer of PSS gives much more homogeneous coating. The first layer of CdS-SO<sub>3</sub><sup>-</sup> reveal aggregates of nanoparticles of up to 50 nm in size. Following deposition steps show an increase in the film roughness and further aggregation of CdS nanoparticles.

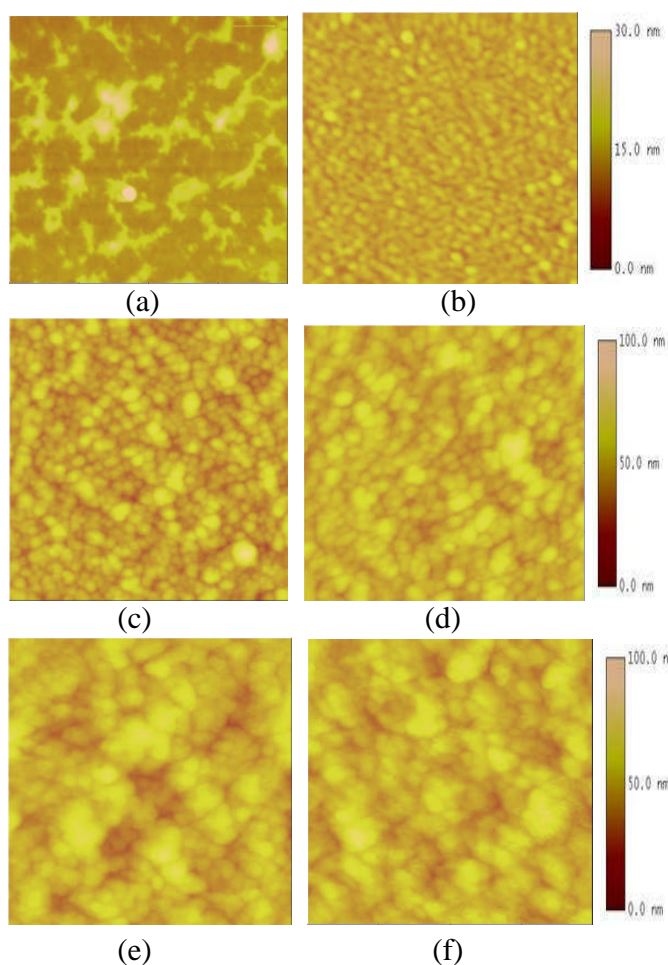


Figure 5. Tapping mode AFM images ( $1\mu\text{m}$  in size) of consecutively deposited layers of: PAH (a), 1<sup>st</sup> PSS (b), 1<sup>st</sup> CdS-NH<sub>2</sub><sup>+</sup> (c), 2<sup>nd</sup> PSS (d), 2<sup>nd</sup> CdS-NH<sub>2</sub><sup>+</sup> (e), and 3<sup>rd</sup> PSS (f)

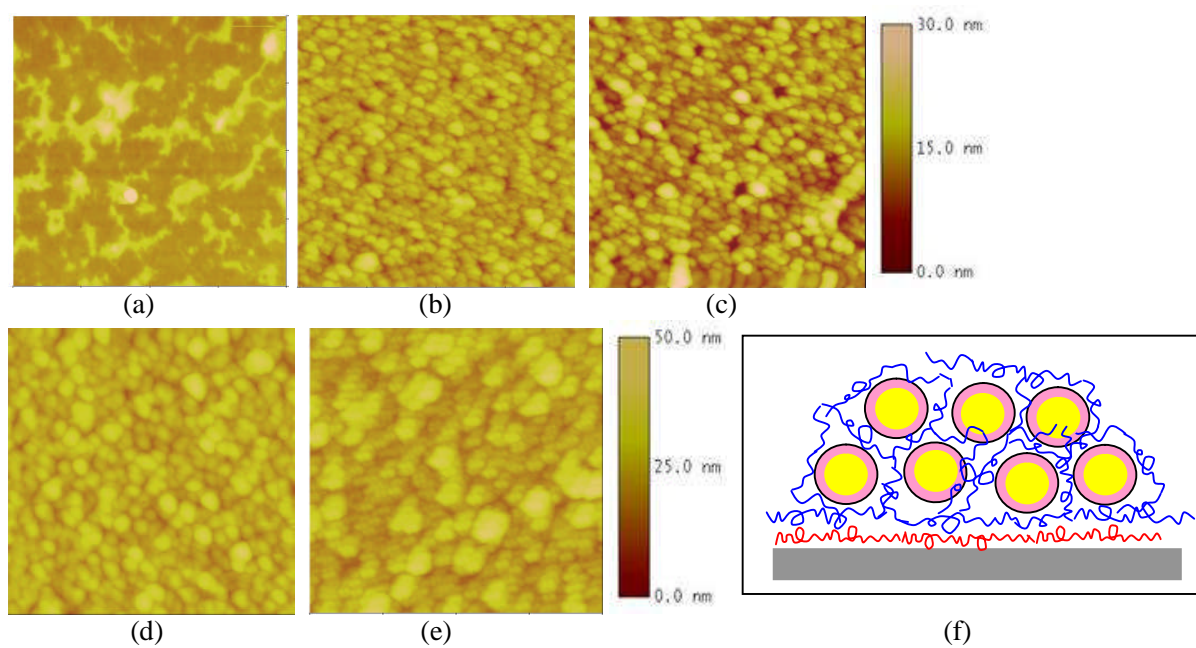


Figure 6. Tapping mode AFM images (1  $\mu\text{m}$  in size) of consecutively deposited layers of: PAH (a), 1<sup>st</sup> ZnS-SO<sub>3</sub><sup>-</sup> (b), 2<sup>nd</sup> PAH (c), 2<sup>nd</sup> ZnS-SO<sub>3</sub><sup>-</sup> (d), and 3<sup>rd</sup> PAH (e). The formation of aggregates of electrically charged nanoparticles by intercalation with polyelectrolytes (f).

A similar situation is observed for PAH/ZnS-NH<sub>3</sub><sup>+</sup> films (see Fig. 6). The roughness of layers and aggregation of ZnS-SO<sub>3</sub><sup>-</sup> increases with the number of layers deposited. The size of ZnS-SO<sub>3</sub><sup>-</sup> aggregates is about 40-50 nm. The aggregation of either positively or negatively charged semiconductor nanoparticles can only happen by intercalation with the layers of polyanions (PSS) or polycations (PAH), respectively, as illustrated schematically by Figure 6(f). This also leads to the increase in the effective thickness of nanoparticle layers often observed for the 2<sup>nd</sup> and following layers deposited.

The aggregation of nanoparticles can be reduced by using diluted colloid solutions. AFM images in Figure 7 show much smaller size of CdS clusters, when the layers were deposited from their diluted colloid solutions. In the case of 500 times dilution, small aggregates of 12-20 nm containing just a few CdS nanoparticles are clearly visible.

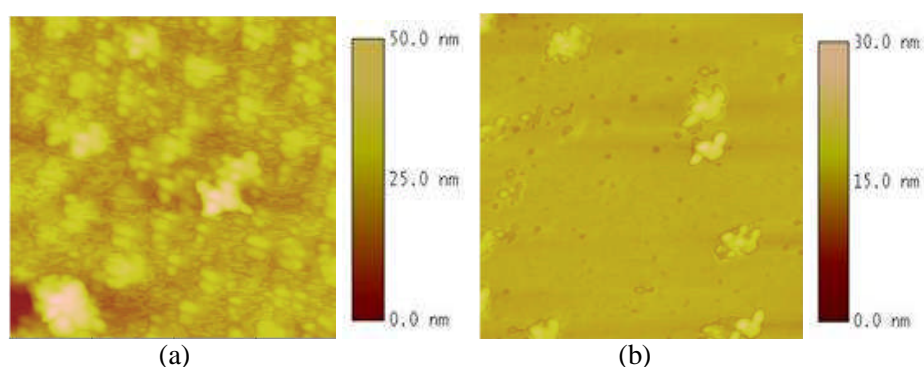


Figure 7. Tapping mode AFM images (1  $\mu\text{m}$  in size) of CdS-NH<sub>2</sub><sup>+</sup> layers deposited from colloid solutions diluted in 100 times (a) and 500 times (b).

## 5. CONCLUSIONS

Multilayers of CdS and ZnS nanoparticles films were successfully deposited onto quartz (glass) and silicon substrates using electrostatic self-assembly via PAH and PSS binding layers. The particle core radius in the range of 1.8 - 1.9 nm for both CdS and ZnS nanoparticles was obtained from UV-vis absorption spectra. Ellipsometry gives slightly larger particle sizes of about 5 nm due to the contribution of the organic shell. AFM shows large (40-50 nm) aggregates of electrically charged nano-particles, which are formed during their adsorption assisted by the intercalation with oppositely charged polyelectrolytes. The size of aggregates can be decreased down to 15-20 nm by diluting colloid solutions.

## REFERENCES

- [1] Nabok A V, Richardson T, Davis F and Stirling C J M 1997 *Langmuir* 13 3198.
- [2] Erokhin V, Facci P, Gobbi L and Dante S 1998 *Thin Solid Film* 327-329 503
- [3] Schwarzacher W, Attenborough K, Michel A, Nabiyouni G and Meier J P 1997 *Journal of Magnetism and Magnetic Materials* 165 23
- [4] Wade T L, Vaidyanathan R, Happek U and Stickney J L 2001 *Journal of Electroanalytical Chemistry* 500 322-332
- [5] Lvov Y and Decher G 1994 *Crystallography Reports* vol. 39 p.628-649.
- [6] Fendler J H 1996 *Chem. Mater.* 8 1616-1624.
- [7] Gao MY, Richter B, Kirstein S 1997 *Adv. Mater.* 9 802
- [8] Gao MY, Richter B, Kirstein S et al. 1998 *J. Phys. Chem. B* 102 4096-4103
- [9] Lesser C, Gao M, Kirstein S 1999 *Mater. Sci. & Eng. C* 8-9 159-162
- [10] Gao, M.Y., Lesser, C., Kirstein, S., et al. 2000 *J. Appl. Phys.* 87 2297-2302

- [11] Winter J. O., Gomez N., Gatzert S., Schmidt C. E. and Korgel B. A., *Colloid and Surfaces A: Physicichem. Eng. Aspects* 254 (2004) 147-157
- [12] Nabok AV, Hassan A K and Ray A K 1999 *Mater. Sci. Eng. C* (8-9) 505-508
- [13] Azzam R M A and Bashara N M 1992 *Ellipsometry and Polarized Light* North-Holland Amsterdam
- [14] Woollam, J A 2002 *Guide to Using WVASE32* J. A. Woollam Co., Inc.
- [15] Yoffe A D 2002 *Advanced in Physics* Vol. 51 No 2 799-890.
- [16] Nabok A V, Richardson T, McCartney C., Cowlam N., Davis F., Stirling C J M, Ray A K, Gacem V and Gibaud A 1998 *Thin Solid Films* 327–329 510